TIFR-BC-85-4
June, 1985

STUDY OF Λ-PRODUCTION IN TARGET FRAGMENTATION REGION FROM pp INTERACTIONS AT 360 GeV/c IN THE TRIPLE REGGE FRAMEWORK

EHS-RCBC Collaboration

Bombay[1], Budapest[2], CERN[3], Chandigarh[4], Genova[5], Innsbruck[6], Japan-UG[7], Madrid[8], Mons[9], Serpukhov[10], Vienna[11] Collaboration.

T.Aziz[1], J.L.Bailly[9], S.Banerjee[1], W.Bartl[11], Yu.Belokopitov[10], F.Bruyant[3], C.Caso[3], Y.Chiba[7(d)], B.Epp[6], A.Ferrando[8], F.Fontanelli[5], S.N.Ganguli[1], T.Gemesy[2], P.Girtler[6], S.Gumenyuk[10], P.Herquet[9], T.Hirose[7(a)], J.Hrubec[3], Y.Iga[7(a)], E.Kistinev[10], V.Kubik[10], J.Macnaughton[11], P.K.Malhotra[1], J.C.Marin[3], M.Markytan[11], S.Matsumoto[7(c)], I.S.Mittra[4], L.Montanet[3], V.Petrovykh[10], G.Pinter[2], P.Porth[11], R.Raghavan[1], M.Regler[11], T.Rodrigo[8], J.Salicio[8], J.B.Singh[4*], S.Squarcia[5], V.Stopchenko[10], K.Takahashi[7(b)], L.A.Tikhonova[**], U.Trevisan[5] and G.Zholobov[10].

(Submitted to Z.Physik C)

1. Tata Institute of Fundamental Research, Bombay, India.
2. KFKI, Budapest, Hungary.
3. CERN, European Organisation for Nuclear Research, Geneva, Switzerland.
4. Panjab University, Chandigarh, India.
5. University of Genova and INFN, Italy.
6. Inst. für Experimentalphysik, Innsbruck, Austria[(+)].
7. (a) Tokyo Metropolitan University, Tokyo, Japan.
   (b) Tokyo University of Agriculture and Technology, Tokyo, Japan.
   (c) Chuo University, Tokyo, Japan.
   (d) Hiroshima University, Hiroshima, Japan.
8. Junta de Energia Nuclear, Madrid, Spain.
9. Universite de lEtat, Faculte des Sciences, Mons, Belgium.
10. I.H.E.P., Serpukhov, U.S.S.R.
11. Inst.für Hochenergiephysik, Vienna, Austria[(+)].

* Now at CERN, Geneva, Switzerland.
** Moscow State University, Moscow, U.S.S.R.

(+) Supported by Fonds zur Förderung der Wissensch. Forschung.

A B S T R A C T

A study of Λ production has been made in the target fragmentation region from pp interactions at 360 GeV/c. The triple Regge analysis of the double differential distribution $d^2N/d(M^2/s)dt$ led to an estimate of the kaon trajectory intercept as ≈ -0.6. Comparison of the double and single inclusive distributions supports the idea of Pomeron factorization. The charged multiplicities and moments from virtual 'K^+'p interactions have been studied as a function of M, the c.m. energy of the virtual 'K^+'p system. The results agree reasonably well with the on shell K^+p data.

1. INTRODUCTION

Several studies have been made in the past for the inclusive production of Λ in the fragmentation region from pp interactions. It is known from triple Regge analyses of pp data upto 69 GeV/c [1-3] and p-Nucleus data upto 300 GeV/c [4,5] that the Regge trajectories responsible for $p \xrightarrow{p} \Lambda$ are strange mesons with strangeness +1 labelled as 'K^+' (for a review see ref. [6]). Since $pp\bar{\Lambda}$ corresponds to exotic quantum number, Mueller Regge picture would indicate the dominance of Pomeron trajectories between proton and $p\bar{\Lambda}$ system. This gives the opportunity of testing factorisation hypothesis for Pomeron using single and double inclusive data. Similar tests have been performed earlier [7] at 100 GeV/c using $p(\bar{p}) \rightarrow \pi^-(\pi^+)\pi^- + X$ data where $\pi^-(\pi^+)$ comes from $p(\bar{p})$ fragmentation region.

In this paper, inclusive production of Λ in pp interactions has been studied in the light of Regge pole picture. Also an attempt has been made to extract information on virtual 'K^+'-proton interactions. The plan of the paper is as follows. Experimental details and data selection are described in section 2. Triple Regge analysis of inclusive unpolarized Λ production in target fragmentation region is presented in section 3. A test of Pomeron factorisation is performed in section 4. Section 5 gives results from a study of virtual 'K^+'-proton interactions and section 6 summarizes the conclusions of the analysis.

2. EXPERIMENTAL DETAIL

The data for this analysis come from an experiment with proton beam at 360 GeV/c on an 80 c.m. Rapid Cycling Bubble Chamber (RCBC) followed by the European Hybrid Spectrometer (EHS) at CERN. Details of the experimental set up are given in the previous papers [8].

The beam is defined by two multiwire proportional chambers. The beam then hits RCBC filled with liquid hydrogen placed in a 3 Tesla magnetic field. The particles produced in the interaction of the protons in the beam with the chamber liquid are detected and momentum analysed in the chamber and the downstream spectrometer. The downstream spectrometer has one multiwire proportional chamber, six drift chambers and a second magnetic field of 1.5 Tesla at about 17.5m away from the centre of RCBC. The spectrometer also has a set of Silica Aerogel Cerenkov counters and a large drift chamber system (ISIS) for particle identification. There are two sets of lead glass detectors (IGD and FGD) to measure the photonic energies in different regions of phase space.

Photographs of the chamber were taken and the electronic signals of the spectrometer were read out when the trigger system (consisting of two sets of scintillator hodoscopes) decides an interaction has taken place. It has been found from simulation studies that this trigger does not lose any interaction except for two prong interactions where the proton goes through either elastic collision or diffractive excitation with a small excited mass. This amounts to 5-6% loss of events with atleast 1 V^0 in RCBC.

A total of 160K pictures was taken. The films were scanned twice using the information of the upstream chamber. This yielded a total of 10672 inelastic interactions containing at least one V^o decay or γ conversion. This sample, which represents ~95% of 160K pictures, corresponds to a sensitivity of ~1.6 events/μb. After measurements the events were processed through HYDRA chain of programs GEOHYB/KINEHS where the kinematic fits of the V^o/γ were carried out.

The total sample of 10672 events yielded 1915 fitted Λ's. By putting a probability cut of 1% and removing all ambiguous fits we are left with 798 unique Λ fits. The efficiency of detecting Λ's is found to be good for Λ's going backward in the c.m. system. Since p-p interaction is symmetric in forward-backward region, we have used for our analysis only uniquely fitted Λ's produced backward in the c.m. system. The Λ's have been corrected for the ambiguous fits and visibility losses.

Events in the target fragmentation region were selected by using a cut in the 4-momentum transfer $|t_{p\Lambda}| = (p_p - p_\Lambda)^2$ as $|t_{p\Lambda}| < 4.0\ GeV^2$; this cut selects Λ's with Feynman $x < -0.2$. No attempt has been made to remove Λ's arising from decays of Σ^0 and Σ(1385).

3. TRIPLE REGGE ANALYSIS

The inclusive reaction $b \xrightarrow{a} c$, with constraints defined by $t=(p_b-p_c)^2$ small, $s=(p_a+p_b)^2$ large, $M^2=(p_a+p_b-p_c)^2$ large and M^2/s small, can be understood in terms of triple Regge diagram. The triple Regge diagram for the case of proton fragmenting to Λ is shown in figure 1. The cross section for unpolarized

Λ production can then be written as

$$\frac{d^2\sigma}{dt\ d(M^2/s)} = \sum_{ijk} G_{ijk}(t).s^{\alpha_k(0)-1}.(M^2/s)^{\alpha_k(0)-\alpha_i(t)-\alpha_j(t)} \qquad (1)$$

where $G_{ijk}(t)$ contains the Regge residues and signature factors. The trajectories α_i and α_j represent strange trajectories K, K_A, K^* and K^{**}. Since $ab\bar{c}$ $(pp\bar{\Lambda})$ is an exotic combination here, the Pomeron term only will dominate for the trajectory α_k. If the intercept of Pomeron is taken as unity, one can simplify eq.(1) as

$$\frac{d^2\sigma}{dt\ d(M^2/s)} = G(t).(M^2/s)^{1-2\alpha_{eff}(t)} \qquad (2)$$

where α_{eff} represents the effective kaon trajectory for $p\bar{\Lambda}$ vertex.

The (M^2/s) distributions in 4-different t-ranges ($-1.0<t<0.0$, $-2.0<t<-1.0$, $-3.0<t<-2.0$, $-4.0<t<-3.0\ GeV^2$) are shown in figure 2. A simultaneous fit has been performed in the four t-bins parametrizing the residue function to be

$$G(t) = A \exp(Bt) \qquad (3)$$

The inclusive cross section corresponding to the bin width can then be written as

$$\sigma = \int_{(M^2/s)_{min}}^{(M^2/s)_{max}} d(M^2/s). \int_{t_{max}}^{t_{min}} dt[A \exp(Bt)][M^2/s]^{1-2\alpha_{eff}(0)-2\alpha'_{eff}t} \qquad (4)$$

Phase space effects for large (M^2/s) values are treated as in reference [9], namely, by calculating t_{min} and t_{max} for a given value of M^2/s and not treating the limits as constants. From a simultaneous fit to the data it is found that the intercept $\alpha_{eff}(0)$ is somewhat correlated with the slope α'_{eff}. We therefore determined the three parameters A, B and $\alpha_{eff}(0)$ for a fixed value of the slope. The results are listed in table 1 for four different values of the slope. For a reasonable value of slope $\alpha'_{eff} \gtrsim 0.8$, the present analysis leads to a value of $\alpha_{eff}(0)=-0.60\pm0.15$. The fitted curves, see fig.2, reproduce the data well for all values of M^2/s.

From the value of the $\alpha_{eff}(0)$ determined above we can predict the shape of the Feynman x distribution. By using the relation $M^2/s=1-|x|$, which is valid for $s\to\infty$ and $|x| > 2s^{-\frac{1}{2}}(p_T^2+M_\Lambda^2)^{\frac{1}{2}}$ with p_T as transverse momentum of Λ, in eq.(2) and integrating over t we get,

$$\frac{d\sigma}{d|x|} = A\,[B - 2\alpha'_{eff}.\ln(1-|x|)]^{-1}.(1-|x|)^{1-2\alpha_{eff}(0)} \tag{5}$$

$$\sim (1 - |x|)^{1-2\alpha_{eff}(0)}$$

$$= (1 - |x|)^{2.2\pm0.3}$$

By fitting the experimental x distribution (not shown) with the above form for $|x| > 0.5$ we get the exponent as 2.2 ± 0.2 which is in good agreement with the predicted value.

Table 2 summarizes the values of the intercepts of the effective kaon trajectory as obtained at different beam momenta. The last row of the table gives the effective kaon trajectory as determined by fitting the energy dependence of inclusive Λ production in pp and $\bar{p}p$ interactions with $p_{lab}>10$ GeV/c [10]. It may be noted from the table that the value of $\alpha_{eff}(0)$ from 69 GeV/c analysis [3] is a little bit positive but with large error compared to other analyses which yield negative values. However, the analyses of the data with nuclear targets [4,5] support the positive value of the intercept. It may be mentioned that these analyses [3-5] do not take into account the phase space effects in M^2/s distributions; the effect of phase space is to make the exponent in $(M^2/s)^{1-2\alpha_{eff}(t)}$ smaller and thus resulting in the overestimation of $\alpha_{eff}(t)$ which will yield higher intercept for the trajectory. Thus we may conclude from the table 2 that the data favour dominance of the unnatural parity kaon trajectory.

4. TEST OF POMERON FACTORIZATION

Mueller Regge theory together with the hypothesis of factorization would enable one to relate two particle inclusive distribution where one particle is produced in beam and the other in target fragmentation region, to single particle inclusive distributions and total cross section [11]. In the target fragmentation region ($|y| \gtrsim 1$), where y is the rapidity of the outgoing particle, one can write the inclusive cross section for Λ and π^- at fixed y and integrated over transverse momentum as (see fig.3)

$$\frac{d\sigma}{dy}(pp \to \pi_b^-) = \beta_P F_P^{p \to \pi^-}(|y|)$$

$$\frac{d\sigma}{dy}(pp \to \Lambda_b) = \beta_P F_P^{p \to \Lambda}(|y|) \qquad (6)$$

We consider only the Pomeron term because the reaction under consideration is exotic. The subscript b refers to backward hemisphere in the cm system. In the case of double fragmentation

$$pp \to \pi_f^- \pi_b^- X$$

$$\text{and} \quad pp \to \pi_f^- \Lambda_b X$$

where the particle with subscript f is produced in the forward hemisphere (projectile fragmentation region) and that with subscript b in the backward hemisphere (target fragmentation region), one can write the double distribution (see fig.3) as

$$\frac{d^2\sigma\,(pp \to \pi_f^- \pi_b^-)}{dy_f dy_b} = F_P^{p \to \pi^-}(|y_f|)\,.\,F_P^{p \to \pi^-}(|y_b|)$$

$$\frac{d^2\sigma\,(pp \to \pi_f^- \Lambda_b)}{dy_f dy_\Lambda} = F_P^{p \to \pi^-}(|y_f|)\,.\,F_P^{p \to \Lambda}(|y_\Lambda|) \qquad (7)$$

From equations (6) and (7), and using factorization hypothesis one gets

$$\frac{d^2\sigma}{dy_f\, dy_b} = \frac{1}{\sigma_{tot}(pp)} \cdot \frac{d\sigma}{dy_f} \cdot \frac{d\sigma}{dy_b} \qquad (8)$$

Instead of using cross sections explicitly one can also use probability functions, and equation (8) can be rewritten as,

$$\omega\,(y_f, y_b\;;\; pp \to \pi_f^- \pi_b^-) = \omega\,(y_f;\, pp \to \pi_f^-)\,.\,\omega\,(y_b;\, pp \to \pi_b^-) \qquad (9a)$$

$$\text{and} \quad \omega\,(y_f, y_\Lambda\;;\; pp \to \pi_f^- \Lambda_b) = \omega\,(y_f;\, pp \to \pi_f^-)\,.\,\omega\,(y_\Lambda;\, pp \to \Lambda_b) \qquad (9b)$$

Figure 4 shows the two sides of formula (9a) for different bins of y_b and plotting them as a function of y_f. The two sets agree rather well within errors (average fluctuation being 4.0% with χ^2 of 1.3 per data point). Figure 5 similarly shows two sides of equation (9b) plotted for two bins of y_f as a function of y . The agreement is again seen to be good as in the previous case. The average fluctuation is 10% with χ^2 of 0.5 per data point. The data thus support the hypothesis of Pomeron factorization. This has been observed in earlier studies with single [12] and double distributions [7] with pions.

5. OFF MASS SHELL 'K⁺' p INTERACTIONS

It has been discussed in section 3 that the events with $|t_{p\Lambda}| \leq 4.0$ GeV^2 have a dominant 'K^+' exchange at the p-$\bar{\Lambda}$ vertex. These events thus represent off mass-shell 'K^+' p interactions with the other proton vertex. The mean charged multiplicity $\langle n_{ch} \rangle$ from these off shell interactions has been plotted in fig.6 as a function of M which is the cm energy of the virtual 'K^+'p system. On the same plot, data from K^+p experiments [13] have been shown. In the overlap region the off mass shell data are in reasonable agreement with the real K^+p data. The solid curve is a fit to the data points with the following expression.

$$\langle n_{ch} \rangle = (1.79 \pm 0.07) + (0.12 \pm 0.05)\ln M^2 + (0.16 \pm 0.07)\ln^2 M^2 \quad (10)$$

The multiplicity moments C_q defined by

$$C_q = \frac{\langle n^q \rangle}{\langle n \rangle^q} \quad (11)$$

have been calculated for q=2 and 3. The values are plotted in figure 7 as a function of cm energy of the 'K^+p' system along with data from K^+p experiments. The values of C_2 agree reasonably well between real and off mass shell K^+p results. There is a slight discrepancy in the trend of C_3 data; the off mass shell data being lower than the real K^+p data. Within errors the values of C_2 and C_3 stay almost constant in the entire energy range indicating the existence of KNO scaling [14] in K^+p interactions.

To study KNO scaling function, one has plotted in fig.8 the quantity

$$\psi_n = \langle n_{ch} \rangle \frac{\sigma_{nch}}{\sigma_{inel}} \quad (12)$$

as a function of $z = n_{ch}/\langle n_{ch} \rangle$ for different values of M. It is seen that within experimental uncertainties the data points from different M ranges seem to fall on a universal curve. This data points agree reasonably well with Slattery parameterization [15] of pp data.

6. SUMMARY

A study of lambda production in the target fragmentation region has been made from 360 Gev/c pp interactions. We have tried to carry out various tests of Regge Mueller picture of inclusive production mechanism. The important features that emerged from the analysis are summarised below:

(1) The distributions for unpolarized Λ production in target fragmentation region can be presented by a triple Regge picture with an effective 'K^+' trajectory of intercept $\simeq -0.6$. From this value of the intercept the shape of the x distribution is predicted to be of the form $(1-|x|)^{2.2 \pm 0.3}$ for large $|x|$ values; the predicted exponent is in good agreement with the data.

(2) Factorisation hypothesis of Pomeron has been tested within ~10% by comparing the inclusive data and correlation data for π^- and Λ production.

(3) Multiplicity moments and KNO scaling function have been studied from the virtual 'K^+'-p interaction upto M value of 23 GeV. It is found that off mass shell results agree in the overlap region with experimental data from K^+p interactions. KNO scaling seems to hold with this new data and also the scaling functions in pp and 'K^+'p data are almost similar.

REFERENCES

[1] V.Blobel et al., Nucl.Phys. B135, 379 (1978).

[2] K.Alpgard et al., Nucl.Phys. B105, 349 (1976).

[3] H.Blumenfeld et al., Nucl.Phys. B125, 253 (1977).

[4] T.Delvin et al., Nucl.Phys. B123, 1 (1977).

[5] F.Abe et al., Phys.Rev. D30, 1861 (1984).

[6] S.N.Ganguli and D.P.Roy, Phys.Rep. 67, 201 (1980).

[7] J.G.Rushbrooke et al., Phys.Rev.Lett. 39, 117 (1977).

[8] J.L.Bailly et al., Z.Physik C22, 119 (1984).
J.L.Bailly et al., Z.Physik C23, 205 (1984).
M.Asai et al., Z.Physik C27, 11 (1985).

[9] S.N.Ganguli and B.Sadoulet, Nucl.Phys. B53, 468 (1973).

[10] S.N.Ganguli, Nuov.Cim.Lett. 20, 554 (1977).

[11] R.C.Brower et al., Phys.Rev. D7, 2080 (1978).

[12] J.Whitmore, Phys.Lett. 60B, 241 (1976).
J.Erwin et al., Phys.Rev.Lett. 33, 1352 (1974).
E.W.Beier et al., Phys.Rev.Lett. 37, 1120 (1976).

[13] J.Whitmore, Phys.Rep. 10C, 273 (1974); Phys.Rep. 27C, 187 (1976).
I.V.Ajinenko et al., Nucl.Phys. B123, 193 (1977).
I.V.Ajinenko et al., Z.Physik C4, 181 (1980).
M.Barth et al., Z.Physik C2, 285 (1979).
W.M.Morse et al., Phys.Rev. D15, 66 (1977).
D.Brick et al., Paper submitted to XIX International Conference on High Energy Physics (1978).

[14] Z.Koba et al., Nucl.Phys. B40, 317 (1972).

[15] P.Slattery, Phys.Rev.Lett. 29, 1624 (1972); Phys.Rev. D7, 2073 (1973).

TABLE 1

Results of triple Regge fit to $\frac{d^2\sigma}{d(M^2/s)dt}$

Fixed slope α'_{eff} (GeV^{-2})	A (GeV^{-2}) (Arbitary normalization)	B (GeV^{-2})	Estimated $\alpha_{eff}(0)$
0.4	$(49.0\pm1.5)\times10^3$	0.72 ± 0.08	-0.8 ± 0.1
0.6	$(51.0\pm1.4)\times10^3$	0.59 ± 0.08	-0.7 ± 0.1
0.8	$(53.8\pm1.5)\times10^3$	0.47 ± 0.08	-0.60 ± 0.15
1.0	$(57.7\pm1.8)\times10^3$	0.35 ± 0.09	-0.60 ± 0.15

TABLE 2

Intercept of the effective kaon trajectory

P_{lab} (GeV/c)	$\alpha_{eff}(0)$	Upper limit of $\|t\|$ used in GeV^2	Reference
12	-0.54 ± 0.07	3.6	[1]
19	-0.38 ± 0.11	4.0	[2]
24	-0.09 ± 0.04	3.6	[1]
69	$+0.20 \pm 0.22$	11.0	[3]
360	-0.60 ± 0.15	4.0	Present Work
>10	-0.20 ± 0.10	---	[10]

FIGURE CAPTIONS

1. Illustration of the triple Regge diagram for $p \xrightarrow{P} \Lambda$.
2. M^2/s distribution for $p \xrightarrow{P} \Lambda$ at 360 GeV/c for different $t_{p\Lambda}$ ranges (a) $-1.0<t<0$, (b) $-2.0<t<-1.0$, (c) $-3.0<t<-2.0$ and (d) $-4.0<t<-3.0$ GeV^2. The fitted curves are described in the text.
3. (a) Single particle inclusive diagram where "c" is in the fragmentation region of the target proton.
   (b) Two particle inclusive diagram where "c" is in the fragmentation region of the target proton and "d" is in the fragmentation of the projectile proton. For the study made in this paper: "c" is π^-_b/Λ_b and "d" is π^-_f.
4. Test of the Pomeron factorization in double and single pion production in pp interactions at 360 GeV/c. Open and closed circles refer to the experimental data pertaining to the L.H.S. and R.H.S. of eq.9(a) of the text.
5. Test of Pomeron factorization using Λ and π^- distributions. Open and closed circles refer to the experimental data pertaining to the L.H.S. and R.H.S. of eq.9(b) of the text.
6. Average charged multiplicity $\langle n_{ch} \rangle$ for virtual 'K^+'p interaction as a function of M - the cm energy of the 'K^+'p system - together with data from on shell K^+p experiments. The fitted curve is described in the text.
7. Multiplicity moments (a) C_2 and (b) C_3 for virtual 'K^+'p interaction as a function of M - the cm energy of the 'K^+'p system-together with data from on shell K^+p experiment.
8. KNO scaling function $\psi_n = \langle n_{ch} \rangle \sigma_{n_{ch}} / \sigma_{inel}$ for virtual 'K^+'p interactions as a function of $z = n_{ch}/\langle n_{ch} \rangle$ for various M - the cm energy of 'K^+'p system. The solid curve represents fit of inelastic pp data [15].

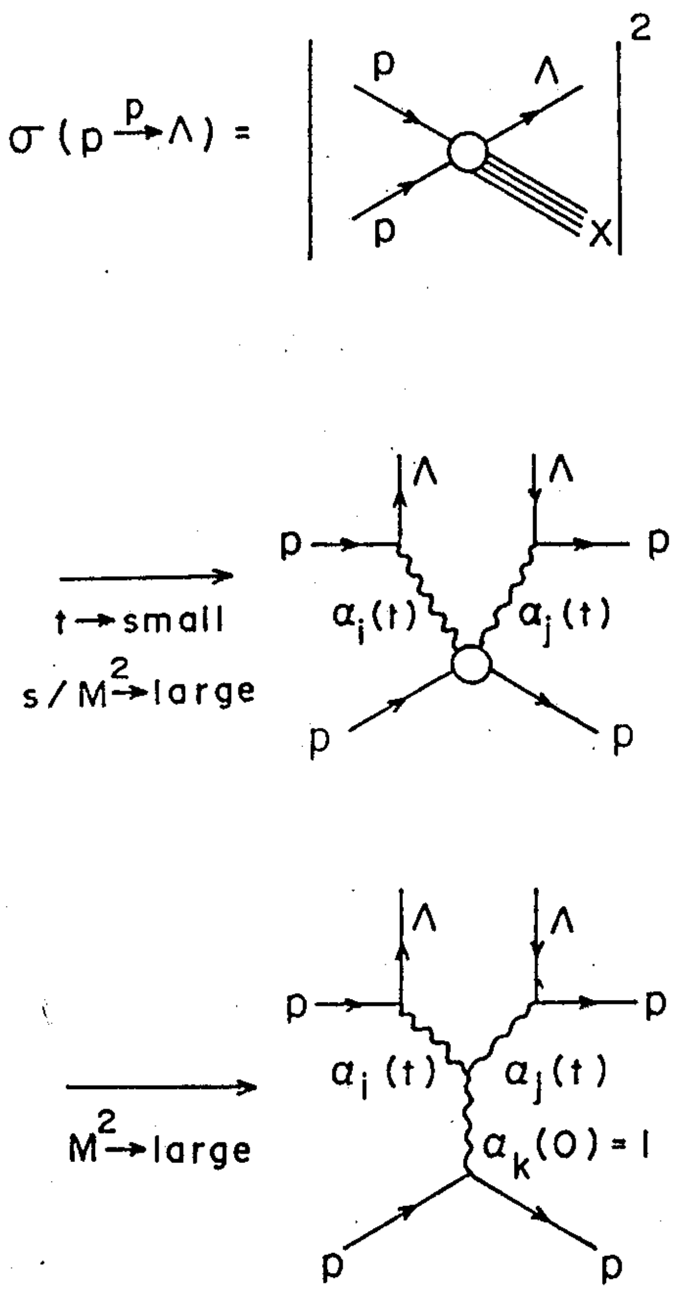
σ (p p→ Λ) =
p
Λ
p
X
2
Λ
Λ
p
p
t → small
s / M2 → large
αi(t)
αj(t)
p
p
Λ
Λ
p
p
αi (t)
αj(t)
M2 → large
αk(0) = 1
p
p

Fig. 1.

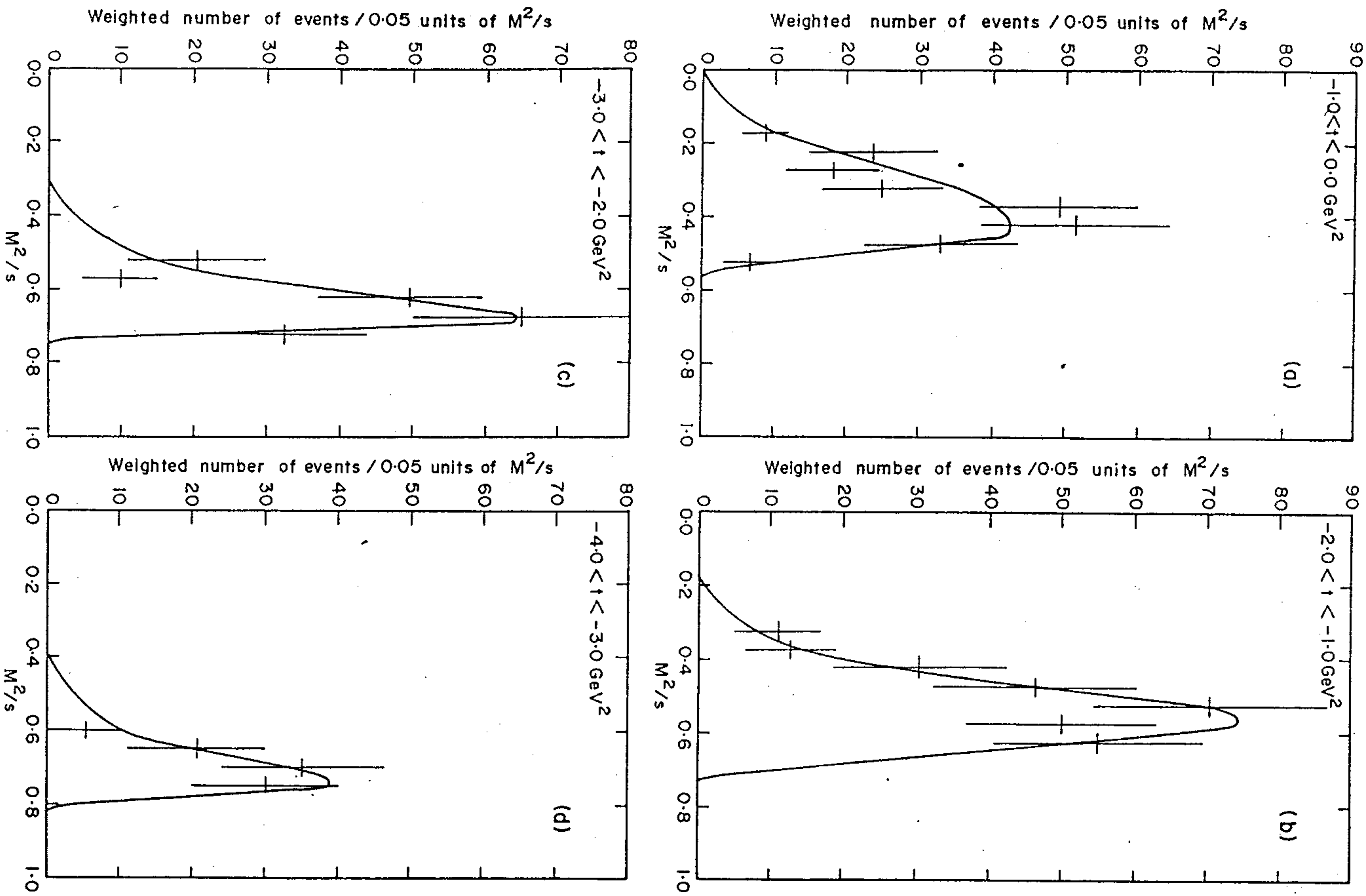
Weighted number of events / 0·05 units of M^2/s
$-1\cdot0 < t < 0\cdot0$ GeV^2
(a)
$-2\cdot0 < t < -1\cdot0$ GeV^2
(b)
$-3\cdot0 < t < -2\cdot0$ GeV^2
(c)
$-4\cdot0 < t < -3\cdot0$ GeV^2
(d)
M^2/s
0·0
0·2
0·4
0·6
0·8
1·0
0
10
20
30
40
50
60
70
80
90

FIG. 2

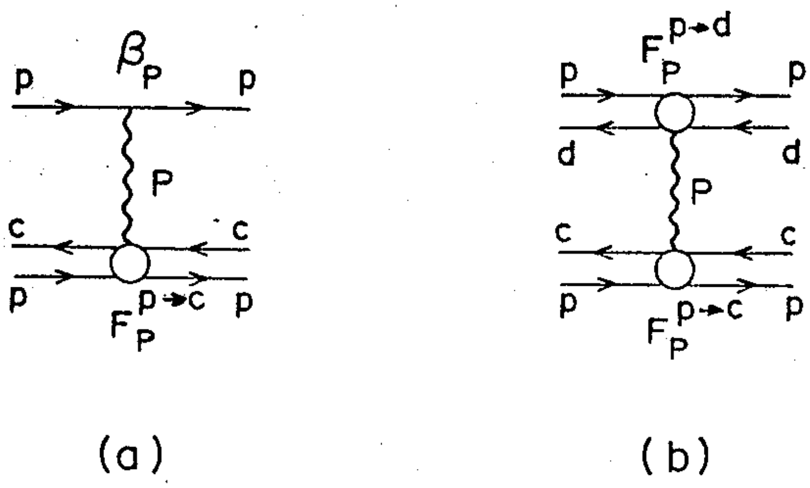

FIG. 3

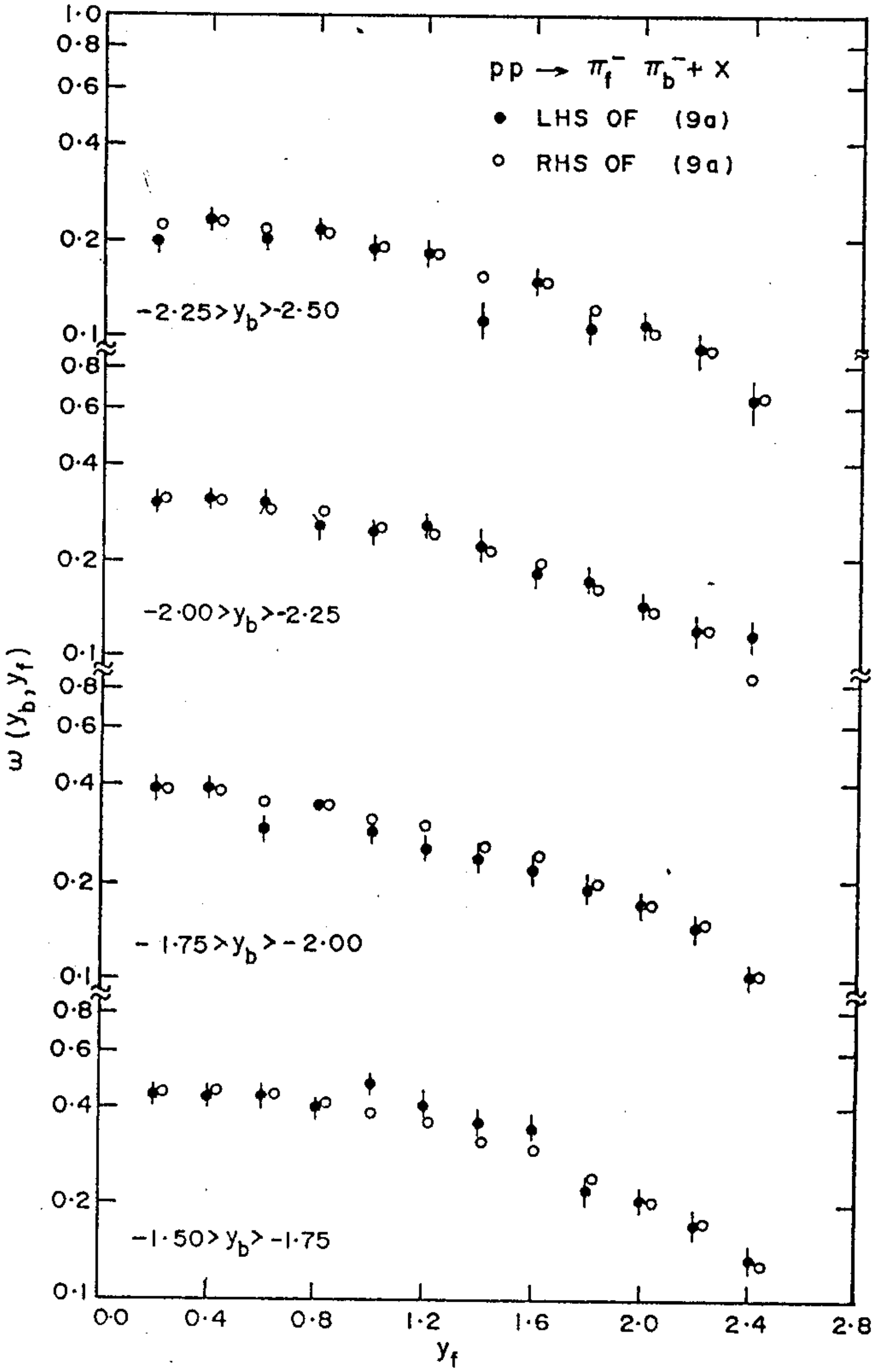

pp → π_f^- π_b^- + X
● LHS OF (9a)
○ RHS OF (9a)
$-2.25 > y_b > -2.50$
$-2.00 > y_b > -2.25$
$-1.75 > y_b > -2.00$
$-1.50 > y_b > -1.75$
$\omega(y_b, y_f)$
y_f
1.0
0.8
0.6
0.4
0.2
0.1
0.0
0.4
0.8
1.2
1.6
2.0
2.4
2.8

FIG. 4

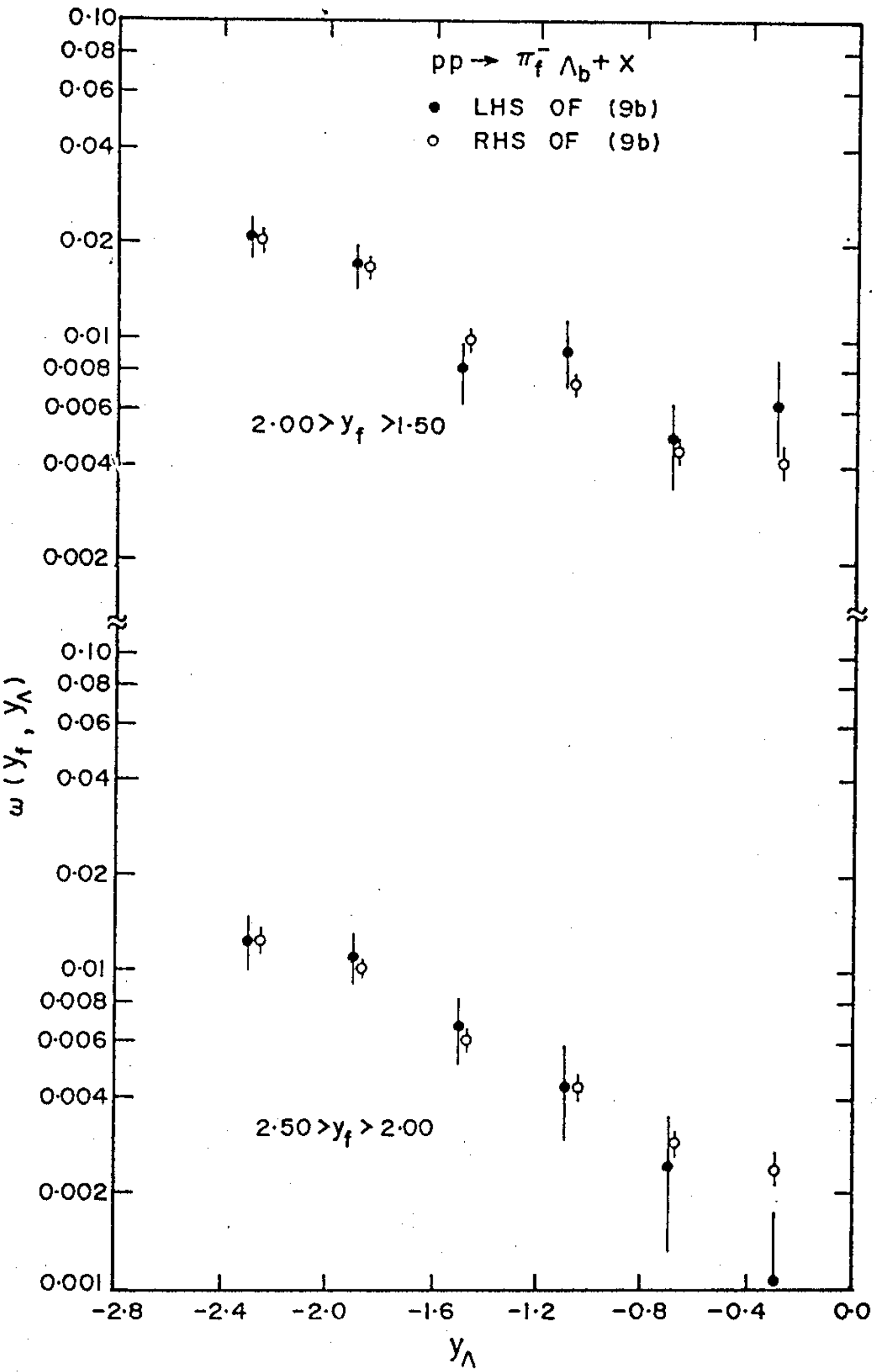

pp → $\pi_f^- \Lambda_b + X$
● LHS OF (9b)
○ RHS OF (9b)
2·00 > y_f > 1·50
2·50 > y_f > 2·00
0·10
0·08
0·06
0·04
0·02
0·01
0·008
0·006
0·004
0·002
0·001
$\omega(y_f, y_\Lambda)$
−2·8
−2·4
−2·0
−1·6
−1·2
−0·8
−0·4
0·0
y_Λ

FIG. 5

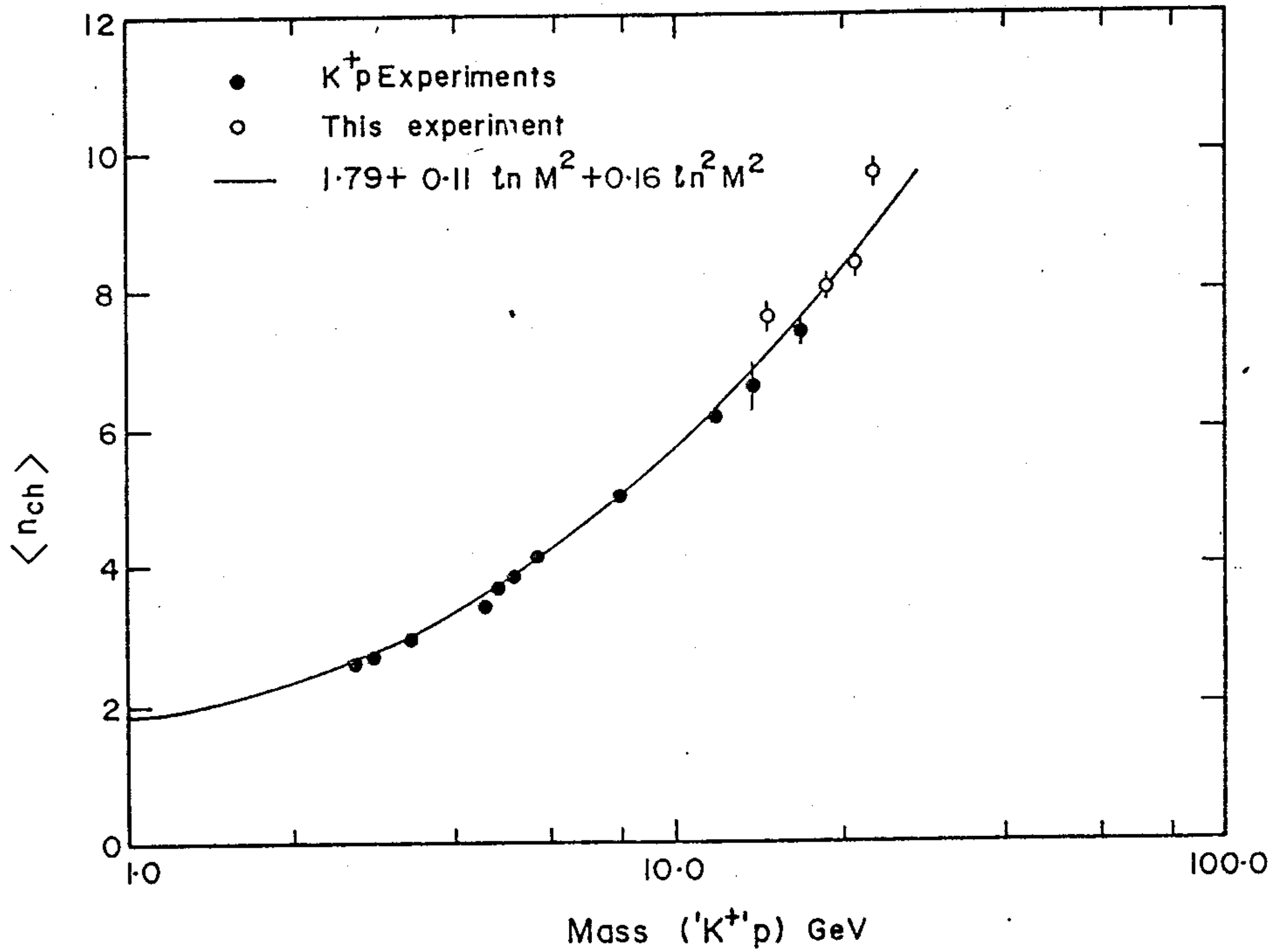

12
10
8
6
4
2
0
⟨n_ch⟩
K⁺p Experiments
This experiment
1·79+ 0·11 ℓn M² +0·16 ℓn² M²
1·0
10·0
100·0
Mass ('K⁺'p) GeV

FIG. 6

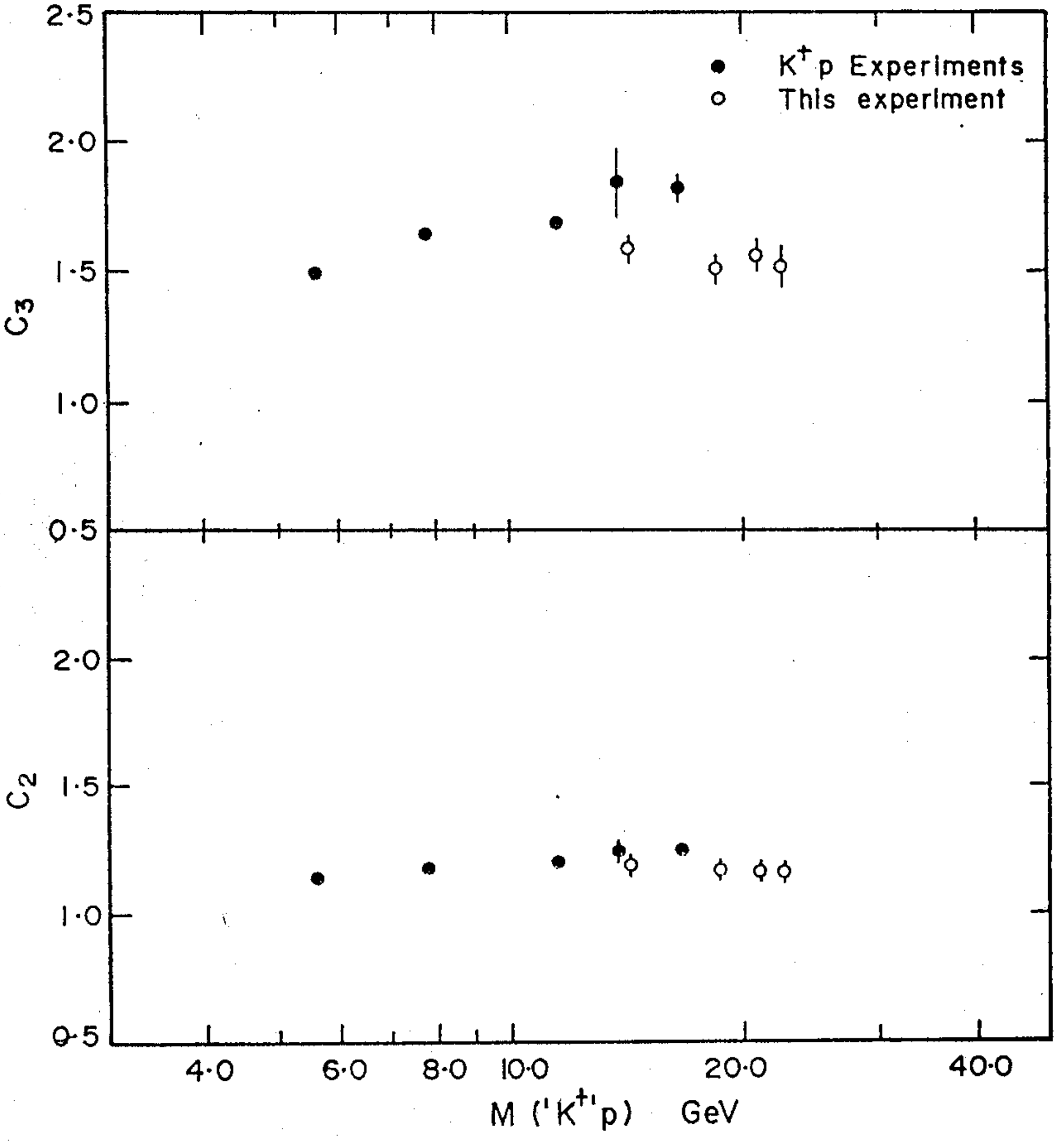
K⁺p Experiments
This experiment
2·5
2·0
1·5
1·0
0·5
C_3
C_2
4·0
6·0
8·0
10·0
20·0
40·0
M ('K⁺'p) GeV

FIG. 7

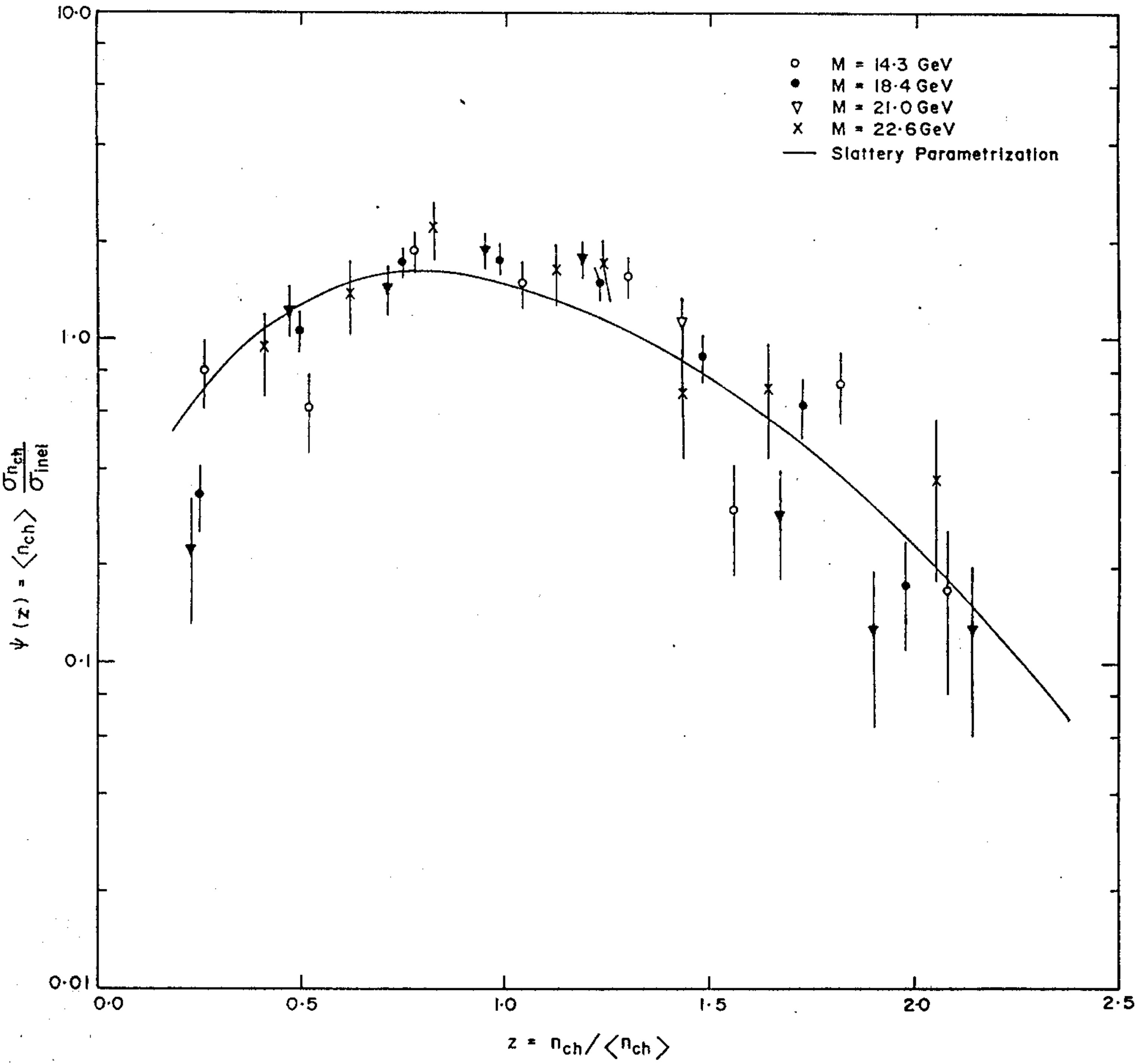

10·0
1·0
0·1
0·01
0·0
0·5
1·0
1·5
2·0
2·5
M = 14·3 GeV
M = 18·4 GeV
M = 21·0 GeV
M = 22·6 GeV
Slattery Parametrization
$\psi(z) = \langle n_{ch} \rangle \frac{\sigma_{n_{ch}}}{\sigma_{inel}}$
$z = n_{ch}/\langle n_{ch} \rangle$

FIG. 8